JOURNAL OF MATERIALS SCIENCE 24 (1989) 3228–3234

Superconducting and mechanical properties of YBCO–Ag composite superconductors

T. NISHIO*, Y.ITOH‡, F. OGASAWARA*, M. SUGANUMA§, Y. YAMADA*¶, U. MIZUTANI*
*Department of Crystalline Materials Science, Nagoya University, Nagoya 464, Japan
‡Aisin Seiki Co., Ltd., Asahimachi, Kariya-shi 448, Japan
§Industrial Research Institute, Aichi Prefectural Government, Nishi-Shinwari, Hitotsugi-cho, Kariya-shi 448, Japan

The measurements of electrical properties and X-ray structural analysis were made for sintered composite materials prepared by mixing the powders of the ceramic superconductor $YBa_2Cu_3O_{7-x}$ (YBCO) and the powders of the pure metal element M with with M = Ni, Cu and Ag at 50 vol% proportions. The superconducting and mechanical properties were studied further on the YBCO–Ag system in the wide volume fractions 0 to 92% Ag. The onset of the superconductivity is found to occur even for samples containing more than 80 vol% Ag. The value of the critical current density is increased initially by adding silver. The mechanical strength against fracture is also improved. The X-ray structural analysis coupled with scanning electron micrographs revealed that silver and YBCO remain intact after sintering and that fine YBCO particles form continuous networks around homogeneously distributed silver particles. This explains well both superconducting and mechanical properties in the present YBCO–Ag composite system.

1. Introduction

The extremely high superconducting transition temperatures of the ceramic superconductors have received particular attention with the hope that they will eventually take over the existing metallic superconducting materials. Indeed, all kinds of efforts have been made from both fundamental and practical points of view. However, there are still a number of difficulties to overcome for practical applications. The brittle nature inherent in ceramics poses one of the most serious difficulties. To overcome this, for instance, the ceramic superconducting material is put in a metal sheath and drawn into a thin composite wire [1, 2]. The chemical reactions and the resulting microstructure, particularly, at the interface between the two materials will determine the superconducting and mechanical properties of the composite system. In any applications of ceramic superconductors, metals are inevitably used as a part of the circuit. Hence, we consider that a basic metallurgical understanding in the ceramic–metal system must urgently be well established. Only limited work has been undertaken so far in an attempt to study the effect of the addition of metal elements to ceramic superconductors [3].

In the present experiments, we have studied, at first, the superconducting properties of sintered composite materials consisting of $YBa_2Cu_3O_{7-x}$ (hereafter referred to as YBCO) and three different metal elements M = Cu, Ni and Ag. From the results thus obtained, further efforts have been focused on the YBCO–Ag system because of its promising superconducting properties. Both superconducting and mechanical properties are evaluated as a function of the volume fraction of silver in YBCO. The metallurgical features characteristic of the YBCO–Ag system are also discussed in relation to the observed microstructures and physical properties.

2. Experimental details

The $YBa_2Cu_3O_{7-x}$ powder, its diameter being less than 150 μm, was purchased from High Purity Chemetals, Japan. The X-ray diffraction pattern can be well indexed in terms of the well-established orthorhombic structure with the lattice constants c = 1.168 nm, a = 0.382 nm and b = 0.389 nm [4]. The powders were pressed into pellets at a pressure of 0.4 GPa and sintered at 1163 K for 12 h in an oxygen-flow atmosphere. The resistivity measurements confirmed the onset of superconductivity at 92 K with a width of 4 K.

The metal powders employed are as follows: silver (99.9%, 100 μm and also a few μm in average diameter), copper (99.99%, a few μm in average diameter) and nickel (99.99%, 100 μm in average diameter). The powders of YBCO and each metal were mixed thoroughly in appropriate proportions and compressed at pressures of 0.4 and 1 GPa at room temperature. The resulting pellets, 20 mm in diameter and 1 mm in thickness, were sintered at 1163 K for 12 h in an oxygen-flow atmosphere with subsequent furnace

¶ Present address: National Research Institute for Metals, Meguro, Tokyo 153 Japan.

0022–2461/89 $03.00 + .12

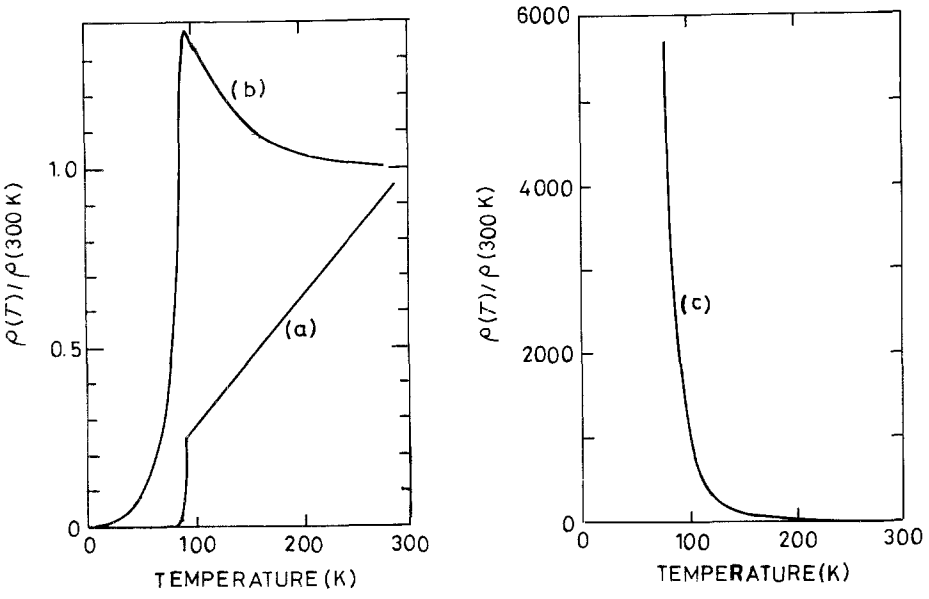

Figure 1 Temperature dependence of electrical resistivity normalized at 300 K for the 50 vol % YBCO–M composites. (a) M = Ag, (b) M = Ni and (c) M = Cu. Note the difference in vertical scale between (a), (b) and (c).

cooling to room temperature. The X-ray diffraction with CuKα radiation was used for structural analysis. In addition, the microstructure was studied with a scanning electron microscope in combination with electron probe microanalysis.

In order to express the content of silver, we employed the volume fraction of silver, rather than its weight percent, as it is more appropriate particularly when composite systems with different metal species are compared on the same footing. The volume fraction is evaluated by assuming the ideal density for each specimen, which is given by the sum of appropriate proportions of crystallographic densities of pure silver ($d = 10.5\,g\,cm^{-3}$) and YBCO ($d = 6.3\,g\,cm^{-3}$). The porosity is defined as $1 - v$, where v is the ratio of the actual measured density over the ideal one defined above. The results are listed in Table I, together with the relevant data.

The electrical resistivity was measured in the temperature range 2 to 300 K, using four-probe d.c. method. The sample for the resistivity measurement was cut into a rectangular shape $1 \times 1 \times 20\,mm^3$ and the current of 10 mA was fed in its longitudinal direction. The current chosen was checked to be sufficiently small for the reliable determination of the critical temperature. The critical current density J_c was determined at 77 K by extrapolating to zero the plot of the generated voltage across the sample against the current. The flexural stress–displacement curve was measured at 300 K in the three-point bending mode with a span of 15 mm and a crosshead speed of $0.5\,mm\,min^{-1}$. A rectangular-shaped sample, $1 \times 3 \times 20\,mm^3$, was employed for the measurements of mechanical properties. Numerical data on electrical and mechanical properties are also summarized in Table I.

3. Results and discussion

3.1. Superconductivity in YBCO–M with M = Ni, Cu and Ag

Fig. 1 shows the temperature dependence of the electrical resistivity for the 50 vol % YBCO–M composite

TABLE I Electrical and mechanical properties of YBCO–Ag composite superconductors

wt % Ag	vol % Ag	density ($g\,cm^{-3}$)	porosity (%)	ϱ ($\mu\Omega\,cm$)	TCR $\times 10^{-3}$ (K^{-1})	T_{c1} (K)	T_{c2} (K)	J_c ($MA\,m^{-2}$)	F (MPa)
P = 0.4 GPa									
0	0	5.2	17	800	2.4	92	88	–	18
25.9	17	5.3	24	500	2.9	92	87	0.68	42
46.7	34	6.3	18	60	3.6	92	84	0.79	45
63.6	50	6.6	21	9	3.7	91	83	0.52	59
77.8	68	8.0	13	4.1	4.0	90	80	0.05	95
84.0	76	8.0	16	3.6	4.0	90	68	*	105
89.7	84	9.5	3	4.3	3.8	90	52	*	132
95.1	92	8.8	14	1.7	3.8	*	*	*	121
P = 1 GPa									
0	0	4.7	25	2400	2.6	92	88	–	42
25.9	17	5.9	16	430	2.9	91	89	1.7	45
46.7	34	–	–	–	–	–	–	1.7	–
63.6	50	7.7	8	11	–	–	–	0.94	106
77.8	68	8.3	10	5	3.6	90	86	0.51	183
84.0	76	–	–	–	–	–	–	–	191
89.7	84	9.1	7	3	3.6	90	35	*	226
95.1	92	9.3	9	2	3.6	*	*	*	210

Note: Columns with * indicate that the measurement is not possible. Columns with – indicate that the measurement has not been made. F in the last column denotes the flexural strength defined in the text.

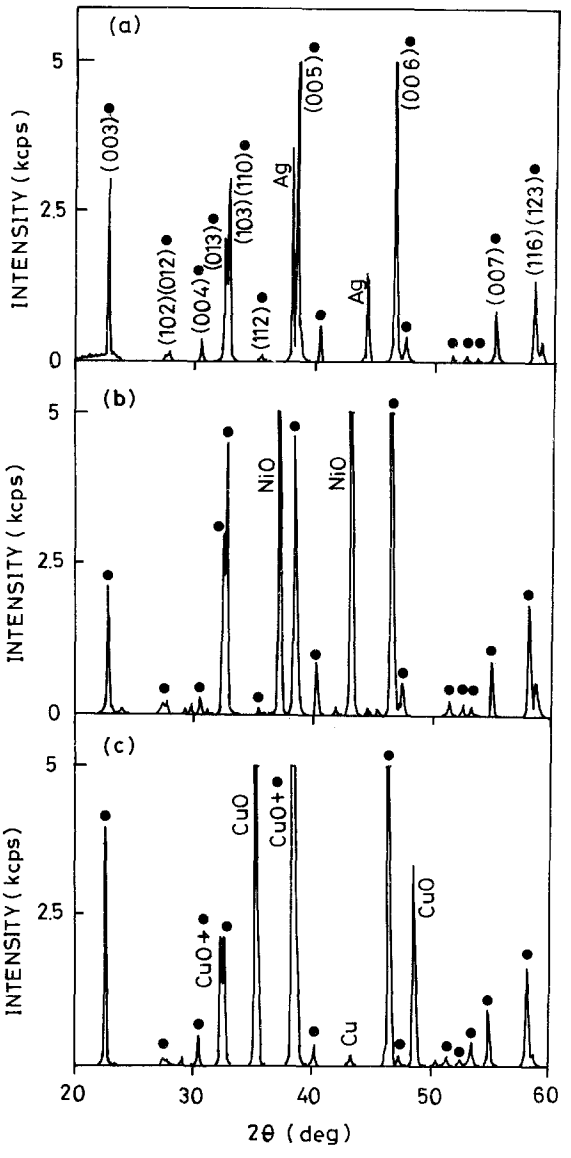

Figure 2 X-ray diffraction patterns for the 50 vol % YBCO–M composites with (a) M = Ag, (b) M = Ni and (c) M = Cu. The diffraction lines for YBCO marked by a symbol ● are indexed in terms of the orthorhombic structure with the lattice constants in the text.

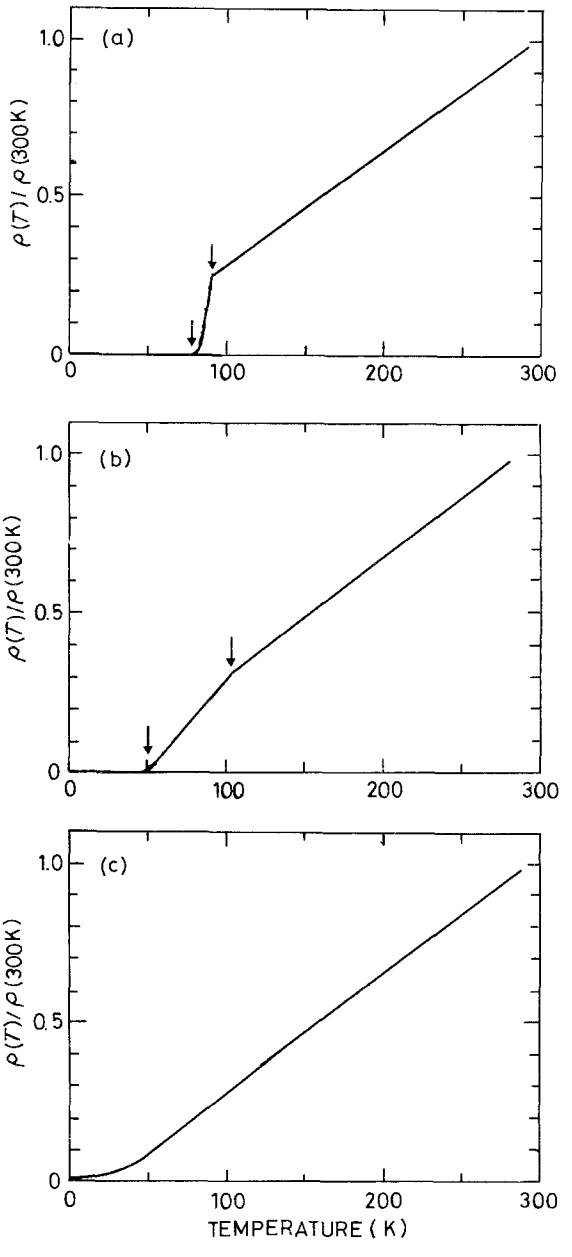

Figure 3 Representative ϱ–T curves for the silver-rich YBCO–Ag composites: (a) 67 vol % Ag, (b) 83 vol % Ag and (c) 92 vol % Ag. All samples shown were pressed at 0.4 GPa before sintering. The arrow indicates the critical temperatures T_{c1} and T_{c2} defined in the text.

samples pressed at 0.4 GPa. The resistivity at 300 K for both YBCO–Ni and YBCO–Cu turns out to be around 10^4 $\mu\Omega$ cm. This is almost 10 times higher than the value of 10^3 $\mu\Omega$ cm for pure YBCO prepared under the same condition. In contrast, the resistivity at 300 K for the YBCO–Ag sample is found to be only 10 $\mu\Omega$ cm. The temperature dependence of the resistivity in Fig. 1 well reflects the magnitude of the resistivity at 300 K: the semiconducting behaviour in both YBCO–Ni and YBCO–Cu, and the metallic behaviour in YBCO–Ag. A sharp superconducting transition occurs in the case of the YBCO–Ag. The sample is, therefore, regarded as a "metal" possessing the superconducting transition temperature of 90 K. On the other hand, a fairly sharp drop in resistivity followed by a long diminishing tail toward low temperatures is observed in the YBCO–Ni sample. Hence, the superconducting path may be more complicated than that in the YBCO–Ag. The resistivity in the YBCO–Cu sample was measured down to 77 K. However, it increased exponentially without any indication of superconductivity.

Fig. 2 shows the X-ray diffraction data for the composite samples YBCO–M identical to those employed for the resistivity measurements in Fig. 1. All diffraction lines for the YBCO–Ag can be identified as the lines arising from pure silver and the orthorhombic YBCO. The c-axis lattice parameter, which is known to be sensitive to the oxygen deficiency [4], is found to remain unchanged relative to that in pure YBCO. This indicates that silver remains intact and that the oxygen deficiency does not occur in YBCO during sintering. In contrast to the YBCO–Ag, the diffraction data for the YBCO–Ni and YBCO–Cu samples show the formation of NiO and CuO with only a small amount of residual pure nickel and copper in the matrix. Nevertheless, it is of interest to note that the diffraction lines for YBCO are essentially unaffected. The formation of metal oxides NiO and CuO in the YBCO–Ni and YBCO–Cu must be responsible for a large increase

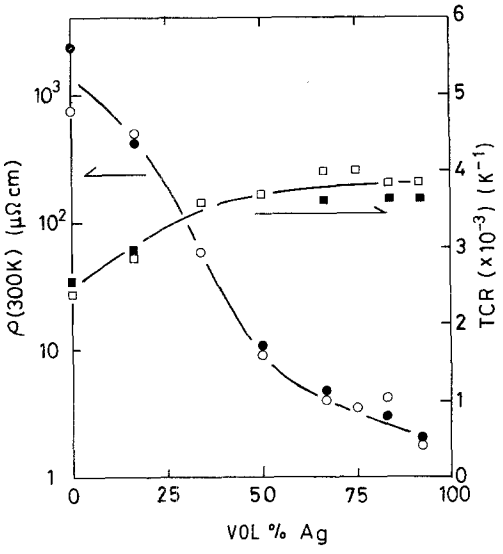

Figure 4 Resistivity at 300 K (○, ●) and TCR (□, ■) as a function of vol % Ag in the YBCO–Ag composites. Open and closed symbols refer to samples pressed at 0.4 and 1 GPa before sintering, respectively.

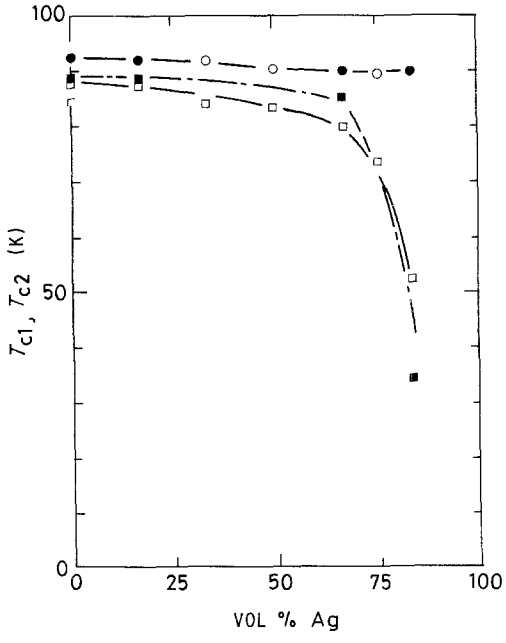

Figure 5 Critical temperatures T_{c1} (○, ●) and T_{c2} (□, ■) as a function of vol % Ag in the YBCO–Ag composites. Open and closed symbols refer to samples pressed at 0.4 and 1 GPa, respectively.

in resistivity at 300 K and for the semiconducting behaviour. In the meantime, we concentrated more detailed studies on the YBCO–Ag system to gain the deeper insight into the superconducting and mechanical properties of this system.

3.2. Superconducting properties of YBCO–Ag

As discussed above, we revealed that a sharp transition at about 90 K can be retained even when one half of a total volume is replaced by the metal powder of silver. This unexpected behaviour has driven us to study the volume concentration dependence of both normal transport and superconducting properties. Some representative ϱ–T data, particularly, for the silver-rich samples pressed at 0.4 GPa are shown in Fig. 3. Superconductivity is observed for all samples except for the one containing more than 90 vol % Ag, which exhibits the residual resistivity at the lowest temperature of 2 K. The value of the temperature coefficient of resistivity (TCR) is calculated from a linear temperature dependence of resistivity above the superconducting transition temperature. The results, along with the resistivity at 300 K, are shown in Fig. 4 as a function of vol % Ag. One can clearly see how the composite sample becomes more metallic with increasing silver content.

With regard to the superconducting properties, we define the two characteristic temperatures T_{c1} and T_{c2} as follows; the former refers to the temperature at which the linearly decreasing ϱ–T curve changes its slope due to the onset of superconductivity and the latter indicates the temperature below which the resistivity vanishes within the resolution of the present experiments. Both T_{c1} and T_{c2} are plotted in Fig. 5 for two series of YBCO–Ag composite samples prepared under two different pressures of 0.4 and 1 GPa. It is clear that the T_{c1} maintains its value above 90 K regardless of silver concentration. The value of T_{c2}, however, begins to decrease sharply when the silver content exceeds about 60 vol %. The results are found to be essentially independent of the pressure employed during sample preparation. More surprising is the fact that zero resistance is achieved below 30 to 50 K even when the silver content is increased above 80 vol %.

The scanning electron micrographs were taken of fractured sections of the YBCO–Ag samples containing various amounts of silver. The micrographs are shown in Fig. 6. First of all, it is found that a bimodal distribution of particle sizes of YBCO exists with a larger one of 20 to 30 μm and a smaller one of less than 5 μm. This is in sharp contrast with a more or less uniform distribution of particle sizes of silver with the average of about 100 μm, indicating that silver particles after sintering maintain essentially the same form as the original ones. The micrograph shows that the fine YBCO particles are distributed uniformly over a large silver particle, forming possibly the three-dimensional network of YBCO. Certainly, the number of YBCO particles decreases and silver particles have more chances to make direct contact with each other with increasing silver content. Nevertheless, the fine YBCO particles tend to cover the surface of the silver particle, keeping the continuous superconducting path over a whole sample. We consider this to be responsible for the persistence of a high T_c value in spite of an extremely large volume fraction of silver.

Based on the scanning electron micrographs in Fig. 6, we propose the microstructure of the YBCO–Ag sintered composite material as schematically illustrated in Fig. 7. We believe that originally small YBCO particles tend to surround the silver particles and form a continuous network during sintering process. An increase in silver content reduces the thickness of the YBCO network around the silver particle while increasing chances for partial contacts between the silver particles. A sharp drop in the resistivity at 300 K with increasing silver content is another evidence for the presence of the direct contact of silver

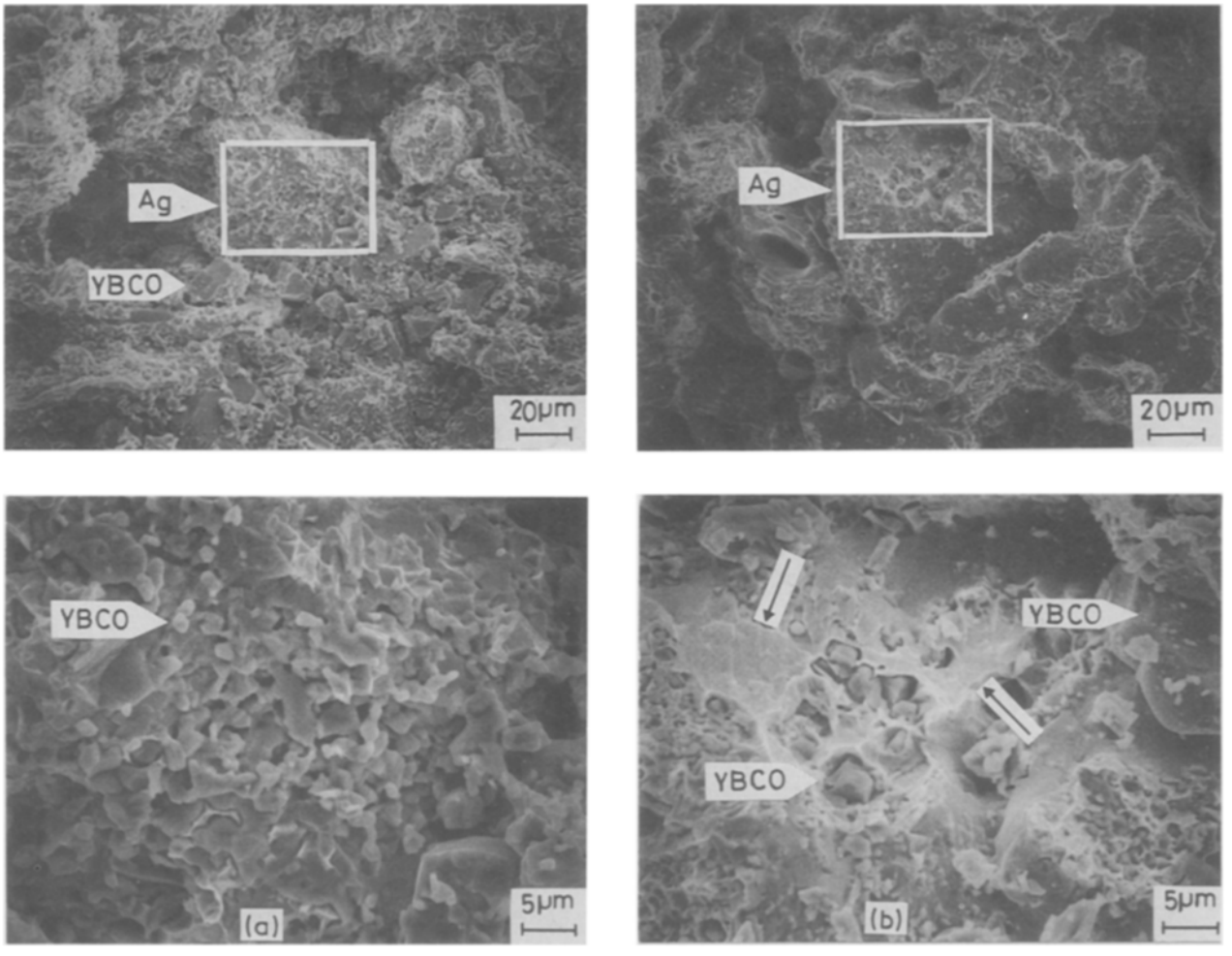

Figure 6 Scanning electron micrographs of fractured surfaces of the YBCO–Ag composite samples containing (a) 50 and (b) 92 vol % Ag, both of which were pressed at 0.4 GPa before sintering. The region surrounded by a white square in each micrograph is enlarged and shown in the bottom. A larger YBCO particle is marked in (a). An enlarged micrograph in (a) shows clearly the formation of the continuous network of YBCO on a silver particle. The silver particle is not seen but EPMA analysis demonstrates its presence underneath. The situation may be seen more clearly in (b), where the amount of YBCO is greatly reduced. An intergranular fracture of a silver particle is also observed as shown by arrows.

particles. Therefore, our interpretation for the superconducting data in Fig. 5 relies on the assumption that the YBCO particles much smaller in size than silver particles must be present as starting materials. To ascertain the sensitive dependence of superconducting properties on the relative size of constituent powders, we prepared the 68 vol % Ag sample using silver powders with the average size less than a few μm. Now small silver particles are distributed homogeneously and independently over a sample and

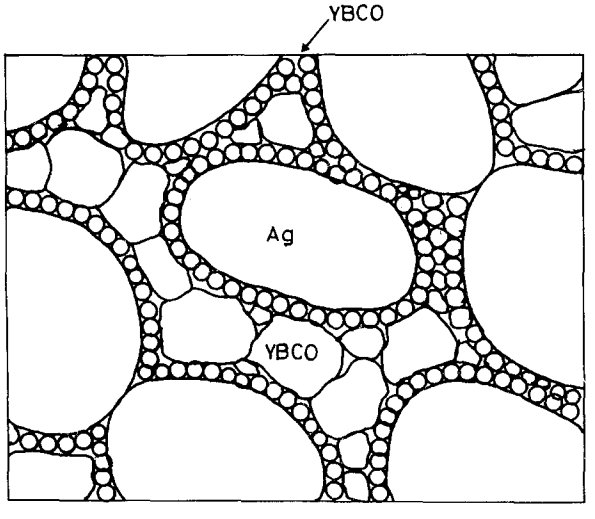

Figure 7 Schematic illustration of the microstructure of the YBCO–Ag composite sample employed in the present experiment. Note the existence of bimodal distributions of YBCO particles (see text).

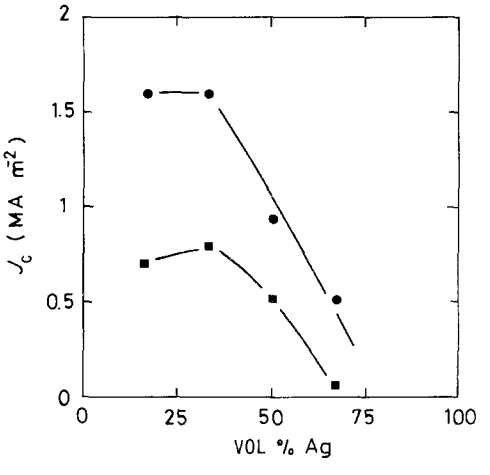

Figure 8 The critical current density J_c as a function of vol % Ag in the YBCO–Ag composites. The data (■) and (●) refer to samples pressed at 0.4 and 1 GPa before sintering, respectively. The value of J_c for pure YBCO is not included here because of the difficulty in obtaining reproducible results. However, we found that the data mostly fell in the range 0.5 to 1 MA m^{-2} regardless of the pressure employed and that an increase in J_c with increasing silver content is definite.

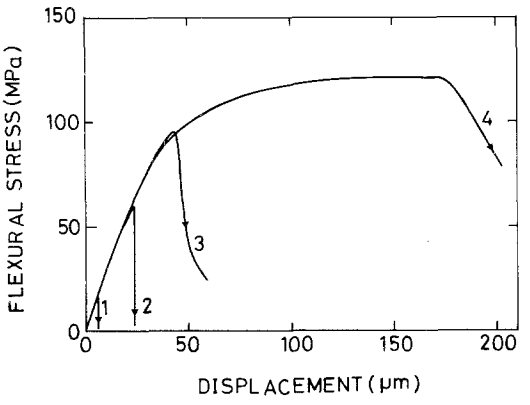

Figure 9 Flexural stress plotted against displacement for the YBCO–Ag composites containing various amounts of silver; (1) pure YBCO, (2) 50 vol % Ag, (3) 67 vol % Ag and (4) 92 vol % Ag. All data shown were taken for samples pressed at 0.4 GPa before sintering.

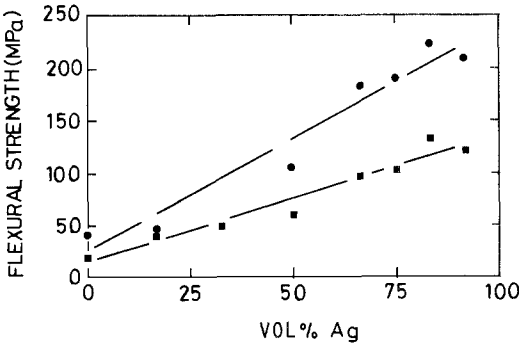

Figure 10 Flexural strength as a function of vol % Ag in the YBCO–Ag composites. The data (■) and (●) refer to samples pressed at 0.4 and 1 GPa before sintering, respectively.

disrupt the superconducting network of YBCO. Indeed, the ϱ–T behaviour is found to resemble that for the 92 vol % Ag samples shown in Fig. 3 without a significant indication of superconductivity down to 2 K.

We turn our attention to the silver concentration dependence of the critical current density J_c measured at 77 K. Here we may reasonably assume that the superconducting current runs only through the YBCO network and essentially bypasses the region of silver particles, provided that the supercurrent due to percolation is less significant. The fraction of area of YBCO in a cross section is simply calculated by assuming that the silver particles are separately and homogeneously distributed in a given volume fraction over a whole volume. The value of J_c is then deduced by dividing the critical current, at which the generated voltage is extrapolated to zero, over the effective cross section thus estimated. The results are shown in Fig. 8. The data for pure YBCO are less accurate and omitted, because Joule heating often took place at the silver paint junction and made the reliable determination of J_c difficult. In contrast, we must emphasize that the determination of J_c for the YBCO–Ag samples is unquestionably easy and reliable, as compared with that for pure YBCO.

We can clearly see from Fig. 8 that the value of J_c strongly depends on the pressure applied in the preparation of a pellet and that it initially increases with increasing silver content. An increase in J_c with increasing applied pressure can be naturally understood such that the fine YBCO particles around the silver particle, which we believe to be responsible for the superconducting path, can form a denser network under increased pressure. On the other hand, an apparent initial increase in J_c with increasing silver content suggests that silver might act as an element to help the formation of a denser YBCO network. A significant decrease in J_c with increase in silver content is most likely attributed to the reduction in the average thickness of YBCO networks.

Before going to the discussion on mechanical properties, we must refer to the reports on studies of electrical properties for YBCO–Ag compounds prepared by the method slightly different from us [5–7]. In these studies, the samples were synthesized by employing as starting materials YBCO and Ag_2O powders, instead of silver metal powders. The persistence of a high T_c value and a sharp drop in resistivity with increasing silver content have been observed [6, 7]. They also reported an increase in J_c with increasing Ag_2O content. Further work is needed to clarify this interesting feature.

3.3. Mechanical properties of YBCO–Ag

Fig. 9 shows the flexural stress as a function of the displacement measured at the centre of the bar samples. It can be seen that the flexural stress initially increases linearly with increasing displacement for all samples studied. The pure YBCO fractures abruptly without plasticity, being typical of a ceramic material. The addition of silver is found to introduce a plastic region, as indicated by a downward bending with increasing displacement, and to increase the flexural strength which is defined as the maximum flexural stress reached in this plot. The flexural stress–displacement curve indicates that the mechanical property essentially resembles that of YBCO, even when the silver content exceeds 50 vol %. This is consistent with our proposed microstructure shown in Fig. 7, since the fracture always takes place along the YBCO network or the "grain-boundary", which is formed around the silver particles. As can be seen in the micrograph in Fig. 6, some silver particles are also fractured. Such a transgranular fracture should be responsible for the plastic behaviour observed in Fig. 9.

The flexural strength is plotted as a function of vol % Ag in Fig. 10 for two series of YBCO–Ag composite samples prepared under different applied pressures. The results indicate that the flexural strength is dependent on the pressure employed and that it increases almost linearly with increasing vol % Ag. We found that a higher pressure is more favourable in terms of J_c and also of the mechanical strength, though it does not measurably affect the value of T_c.

3.4. Soldering with lead wires

One of the drawbacks of ceramic superconductors stems from the difficulty in making a direct contact with lead wires by soldering. We tried to solder a copper lead wire directly on the YBCO–Ag sample. The soldering can be perfectly made, particularly when silver content exceeds about 50 vol %. The

electrical connection was found to be stable down to liquid helium temperatures.

In conclusion, we have studied the superconducting properties of composite systems YBCO–M with M = Ni, Cu and Ag and found that the YBCO–Ag system is the most appropriate from the point of view of its promising superconducting behaviour. Detailed studies revealed that silver particles remain intact and, hence, keep their original forms without involving partial melting or coagulation during the sintering process at 1163 K. On the other hand, the fine YBCO particles tend to surround the silver particle and form a three-dimensional dense network. This explains well both superconducting and mechanical properties in the YBCO–Ag composite system. The present results also provided the idea that the poor mechanical property inherent in ceramic superconductors can be substantially improved by forming composites with silver powders, while keeping or even improving superconducting properties required for practical application. Further efforts should be made to optimize the size and shape of silver particles and its volume ratio relative to YBCO powders, in order to attain the best superconducting and mechanical properties in the YBCO–Ag composite system.

References

1. O. KOHNO, Y. IKENO, N. SADAKATA and K. GOTO, *Jpn J. Appl. Phys.* **27** (1988) L77.
2. R. FLÜKIGER, T. MÜLLER, W. GOLDACKER, T. WOLF, E. SEIBT, I. APFELSTEDT, H. KÜPFER and W. SCHAUER, *Physica C* **153–155** (1988) 1574.
3. S. JIN. R. C. SHERWOOD, T. H. TIEFEL, G. W. KAMMLOTT, R. A. FASTNACHT, M. E. DAVIES and S. M. ZAHURAK, *Appl. Phys. Lett.* **52** (1988) 1628.
4. A. ONO and Y. ISHIZAWA, *Jpn J. Appl. Phys.* **26** (1987) L1043.
5. Y. SAITO, T. NOJI, A. ENDO, N. HIGUCHI, K. FUJIMOTO, T. OIKAWA, A. HATTORI and K. FURUSE, *ibid.* **26** (1987) L832.
6. V. PLECHACEK, V. LANDA, Z. BLAZEK, J. SNEIDR, Z. TREJVALOVA and M. CERMAK, *Physica C* **153–155** (1988) 878.
7. D. PAVUNA, H. BERGER, J. -L. THOLENCE, M. AFFRONTE, R. SANJINES, A. DUBAS, PH. BUGNON and F. VASEY, *ibid.* **153–155** (1988) 1339.

Received 15 August
and accepted 3 November 1988